ELSEVIER

International Journal of Mass Spectrometry 185/186/187 (1999) 37–47

International Journal of Mass Spectrometry

Influence of solvent composition and capillary temperature on the conformations of electrosprayed ions: unfolding of compact ubiquitin conformers from pseudonative and denatured solutions

Jianwei Li, John A. Taraszka, Anne E. Counterman, David E. Clemmer*

Department of Chemistry, Indiana University, Bloomington, IN 47405, USA

Received 16 April 1998; accepted 4 August 1998

Abstract

High-resolution ion mobility/mass spectrometry methods have been used to examine the influence of solvent composition and capillary temperature on the gas-phase conformations of ubiquitin ions (+6 to +13) formed during electrospray ionization. Three general conformer types are observed: compact forms (favored for the +6 and +7 charge states); partially folded conformers (favored for the +8 and +9 ions); and, unfolded conformers (favored for the +10 to +13 charge states). The populations of different conformers are highly sensitive to solvent composition and capillary temperature used for electrospray ionization. Electrospray of "pseudonative" solutions leads to formation of some conformers that are more compact than those observed for "denatured" solutions. Studies as a function of capillary temperature show that as the capillary temperature is increased, compact and partially folded states undergo unfolding transitions. Compact states from pseudonative solutions unfold at higher temperatures than compact states from denatured solutions. The products of unfolding transitions have similar cross sections for both solution types. (Int J Mass Spectrom 185/186/187 (1999) 37–47) © 1999 Elsevier Science B.V.

Keywords: Ubiquitin; Electrospray; Temperature; Solvent; Ion mobility

1. Introduction

A number of mass spectrometry based methods are currently being developed to examine the conformations of protein ions. These include: measurements of collision cross sections by ion mobility [1–4] and ion scattering methods [5]; kinetic energy release measurements [6]; microscopy studies of surfaces bombarded with high energy ions [7]; measurements of gas-phase H/D exchange levels [8–11] and gas-phase basicities [12]; and studies of adduct formation [13, 14]. Mass spectrometry methods offer a means of studying proteins in well-defined environments; specified numbers of attached protons and solvent molecules can be defined by a selection of mass-to-charge ratios. Studies of anhydrous ions and protein–solvent adducts in the gas phase are useful in determining the roles of intramolecular and solvent–molecule interactions in establishing conformation.

A limitation in comparing structural information for biomolecular ions formed by electrospray ionization (ESI) [15] is that different ESI source conditions (i.e. solvent composition; capillary temperature; pressures, voltages, and distances in interfacial pressure

* Corresponding author.

Dedicated to Professor Michael T. Bowers on the occasion of his 60th birthday.

PII S1387-3806(98)14135-0

regions) are often used. Source parameters that control ion formation will most likely also influence the conformation of the gas phase ions. Several studies have suggested that ions may retain some degree of "memory" in the gas phase [4b,5a,7,16,17]. It is well known that factors such as pH [18], solvent composition [19], and temperature [20–22] influence the distribution of charge states formed by ESI. In this article we have investigated the influence of solvent composition and capillary temperature upon conformations of ubiquitin ions formed by ESI in a high pressure ion mobility instrument. In this instrument, ions are formed and probed at high pressures without exposure to energetic collisions that can occur in interfacial regions of the mass spectrometer. The approach is sensitive to variations in source conditions that influence gas-phase conformation. Using this method, Jarrold and co-workers have recently shown that ion mobility distributions for selected cytochrome *c* charge states are influenced by the solution composition and have suggested that the approach may be important as a tool for examining solution phase conformations [16]. The results that we present here show that gas-phase ions formed from solutions that we refer to as "pseudonative" (i.e. solution compositions where water comprises more than ~90% of the solution) favor gas-phase conformations that are more compact than ions formed from solutions that are referred to as "denatured" (solutions comprised of more than 30% of a nonaqueous solvent). When the capillary temperature is increased, partially folded and unfolded conformers are formed. These ions have similar cross sections for both solvent systems, but the temperature required to unfold compact states from the pseudonative solutions are higher than for denatured solutions. Overall, the results presented here show that in order to make reasonable comparisons of structural data obtained in different laboratories it is important that the conditions used to form ions are well characterized.

Ubiquitin is a small cytoplasmic protein (76 amino acids) that contains no disulfide bonds [23]. In solution it is stable with respect to unfolding in the temperature range of 23 to 80 °C and over a pH range of 1.18 to 8.43 [24,25]. Unfolded forms dominate for solution compositions containing ~40% or more of mild denaturants such as methanol [26]. Our previous measurements of cross sections for the +6 to +13 charge states formed directly by ESI show that it is relatively free to adopt a wide range of folded, partially folded and unfolded conformations with cross sections ranging from ~1000 to 1950 Å^2. Cassady and co-workers [10,27] have examined the proton-transfer reactivity of ubiquitin with different bases and reported apparent gas-phase acidities for different charge states [27]. We investigated conformations of proton transfer product ions and determined the relative magnitudes of apparent gas-phase acidities for different conformations within a given charge state; compact < partially folded < elongated [4c]. Smith and co-workers have shown that variations in solution composition (which should favor native or denatured ubiquitin states) resulted in different charge state distributions upon ESI [9a]. However, no differences in the proton transfer reactivity of these ions were observed.

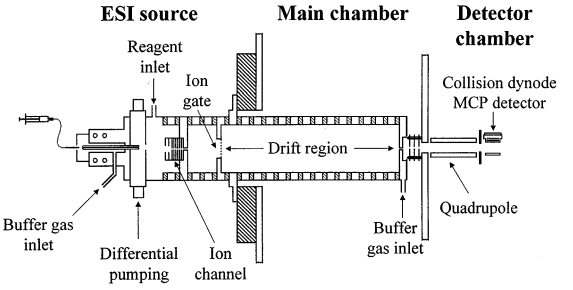

Fig. 1. Schematic diagram of the high-resolution ion mobility apparatus used in these studies.

2. Experimental

2.1. General

The high-resolution ESI-ion mobility instrument used in these studies is similar to several that have been described recently [16,28]. A schematic diagram of the experimental apparatus is shown in Fig. 1. Ion mobility distributions for specific charge states were

obtained by recording the time required for a pulse of ions to drift through a drift tube filled with inert buffer gas under the influence of a uniform electric field. Different conformations are separated because of differences in their mobilities through the buffer gas. Compact conformations (with relatively small collision cross sections) have higher mobilities than elongated conformations. Ions that exit the drift tube are focused into a quadrupole mass spectrometer that can be fixed to transmit a specific mass. Ions are detected using an off-axis collision dynode/microchannel plate detection system.

2.2. Variable temperature ESI source

Ubiquitin (bovine, Sigma, 90%) ions are formed by electrospraying solutions containing 3 to 8×10^{-5} M protein. Solution compositions ranging from 9:89:2 to 94:4:2 water:acetonitrile:acetic acid were used. Droplets are electrosprayed at atmospheric pressures directly into a variable temperature stainless steel capillary tube. The capillary has an inner diameter of 0.15 cm and is 18.5 cm long. The entrance of the tube protrudes into a Plexiglas chamber that can be pressurized with He gas as shown in Fig. 1. Ions are forced through the tube by a pressure drop that results from differential pumping at the exit of the capillary. The capillary is in thermal contact with an aluminum block that can be heated with cartridge heaters or cooled by flowing liquid nitrogen through the block. The temperature of the capillary is measured using a thermocouple. The temperatures that are reported are for the inside surface of the capillary at the exit end. Temperatures were calibrated in a separate experiment and have uncertainties of ± 5 °C.

2.3. Reaction cell

Ions exit the capillary and differential pumping region and enter a reaction cell where reagents can be introduced. The reaction cell was not used in the experiments presented here. The background gas pressure (comprised of primarily He and some ambient laboratory air) in the reaction cell was ~150 to 200 Torr. Ions drift ~3 cm through this region under the influence of a weak electric field; based on the distance, pressure, and mobilities measured below, we estimate that ion residence times in this region are ~3 to 30 ms for the different charge states, conformations, and electric field strengths used.

2.4. High-pressure drift region

Ions exit the reaction cell under the influence of an electric field created by 10 BeCu rings that are separated by Teflon rings and connected by a series of high vacuum resistors (5 MΩ, 1%, KDI Electronics). The rings and spacers create a 0.2 cm diameter channel that is ~2.5 cm long and the voltage drop across this region is ~1000 to 2000 V. Most of the He buffer gas that is added to the drift tube region is pumped away through this channel. The electric field guides ions into the body of the drift tube against the counterflow of the He buffer gas, while preventing neutrals from entering the drift region. Once inside the body of the drift tube, the ions drift through the buffer gas under the influence of a field provided by the copper ring electrodes until reaching a wire gate, similar to one described by Hill and co-workers [1d]. The gate was constructed by stringing wire (nickel/iron alloy) to form sets of alternating, parallel rows spaced 0.07 cm apart on a fiberglass support. Opposite polarity voltages (± 30 to 200 V) are applied to the wires in order to introduce pulses (50 to 100 μs) of ions into the drift tube. The drift region is 48.74 cm long and is created by a series of 2.5 cm thick copper rings (10.2 and 15.2 cm inner and outer diameter, respectively) separated by 1.27 cm thick ceramic spacers machined from mycalex (McMaster Carr). The copper/mycalex ring system is sealed by indium or silver wire, or viton O-rings, creating a cavity that can be filled with buffer gas. The drift field is generated by voltages applied to the copper rings. In these studies drift fields of ~50 to 250 V cm^{-1} were used. Calculations of the equipotential lines [29] created using this geometry show that the drift field is highly uniform along the

drift axis, an important criterion for recording high-resolution ion mobility distributions [1d]. Plots of drift velocity against drift voltage are linear over the range of electric fields used. This indicates that ions drift through the instrument in the "low-field limit," where they are expected to sample all possible orientations and have internal energies that are thermalized by collisions with the buffer gas. Reduced mobilities recorded with this instrument for a wide range of different ions, including peptides [30], oligonucleotides [31], and different protein charge states are in good agreement (within 2% relative uncertainty) of data recorded in our injected ion instrument [4,32] and are usually in good agreement with data from other laboratories [3,33].

2.5. Ion mobility and collision cross section distributions

The time required for a pulse of ions to reach the detector is a composite of the drift time, and time required for ions to travel through other portions of the instrument. Thus, it is necessary to account for the flight times of ions when no buffer gas is present, as well as for differences in the ions' energies at the exit of the drift tube in the presence and absence of buffer gas. These corrections are small (~150 to 250 μs) in these experiments. The time axis of drift time distribution plots can be converted into a cross section axis by the relation [2]

$$\Omega = \frac{(18\pi)^{1/2}}{16}\frac{ze}{(k_bT)^{1/2}}\left(\frac{1}{m_u}+\frac{1}{m_{\mathrm{He}}}\right)^{1/2} \times \frac{E}{L}\frac{760}{P}\frac{T}{273.2}\frac{1}{N}\times t_D \quad (1)$$

where t_D is the drift time, E is the electric field, P is the pressure of the buffer gas, z is the charge state, N is the neutral number density, and m_u and m_{He} are the masses of ubiquitin (8565) and He (4), respectively. Display of data as cross section distributions is useful for comparison of different charge states.

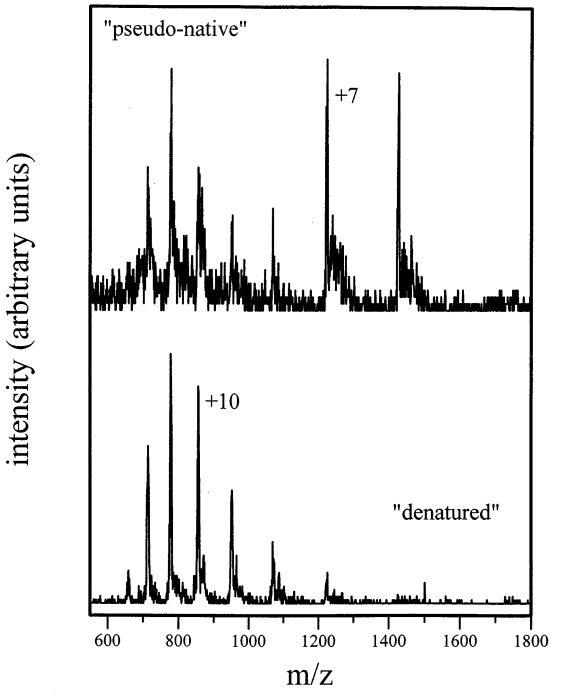

Fig. 2. Mass spectra for ubiquitin ions formed upon electrospraying 49:49:2 (denatured) and 89:9:2 (pseudonative) water:acetonitrile: acetic acid solutions.

3. Results and discussion

3.1. Solvent composition and gas-phase conformation

Mass spectra and cross section distributions were obtained for ions that were electrosprayed from solutions comprised of varying compositions of water and acetonitrile and a fixed amount of acetic acid. Solution compositions ranging from 9:89:2 to 94:4:2 water:acetonitrile:acetic acid (% volume) were used. Mass spectra for two representative solvent compositions (49:49:2 and 89:9:2 water:acetonitrile:acetic acid) are shown in Fig. 2. The charge state distribution recorded for the 49:49:2 solution is dominated by the +11 charge state. ESI of the 89:9:2 solution leads to a mass spectrum that shows a bimodal distribution of charge states. The +9 to +13 charge states have similar relative intensities to those observed from the 49:49:2 solution; in addition, there is a substantial

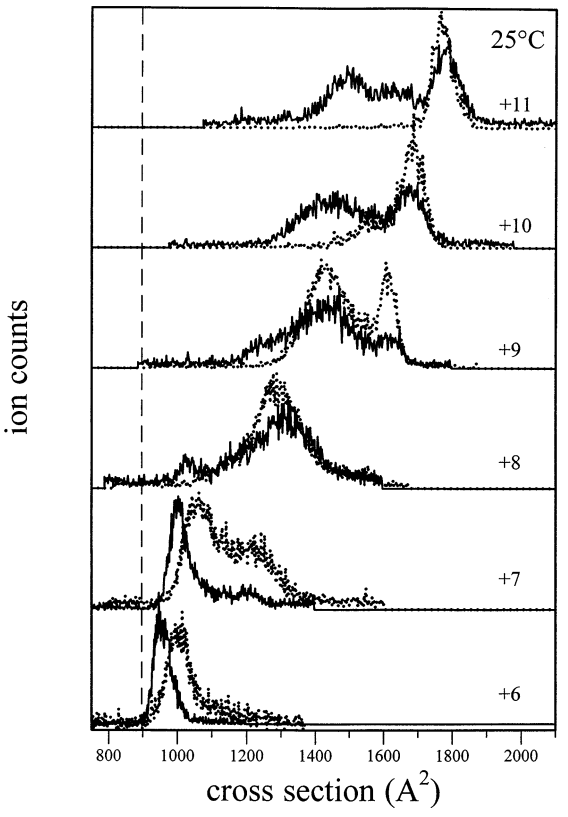

Fig. 3. Cross section distributions (see the text) for the +6 to +11 charge states of ubiquitin obtained by electrospraying a 49:49:2 water:acetonitrile:acetic acid solution (solid circles) and a 89:9:2 water:acetonitrile:acetic acid solution (solid lines). These data were recorded at a source capillary temperature of 25 °C. The dashed line shows the calculated cross section for the crystal coordinates of ubiquitin, taken from Ref. 34.

increase in the relative abundances of the +6 to +8 charge states. The differences in these mass spectra upon varying the solution composition are similar to data reported previously for ubiquitin [19] and other proteins [18,20–22]. In the following, we refer to solutions comprised of at least 89% water as pseudo-native (*N*) and solutions containing less than ~70% water as denatured (*D*).

Cross section distributions for the +6 to +11 charge states recorded for *D* and *N* solutions are shown in Fig. 3. These ions were formed by electrospraying ions into a 25 °C capillary. The cross section distributions for the +6 ions from both solutions show single peaks at 950 Å^2 (*N*) and 1000 Å^2 (*D*). These values are near the 897 Å^2 cross section we have estimated previously [4c] for the crystal coordinates of ubiquitin [34] calculated by the projection approximation [3b, 4b]. Cross section estimates from the projection method ignore long-range interactions between the ions and buffer gas as well as the scattering dynamics [35,36]. The 897 Å^2 is best viewed as a lower limit to the actual cross section [2]. The similarities of the experimental cross sections and the calculated value for the +6 ions indicate that conformations from both solutions are highly folded. The observation that ions from the *N* solution have conformations that are more compact than those from the *D* solution indicate that gas-phase ion conformation is influenced by the solvent system used for ESI. This is discussed in more detail below.

Cross section distributions for higher charge states formed from both solutions show that ions expand with increasing charge state. The +7 N distribution is dominated by ions with cross sections that are centered at ~1000 Å^2 and a smaller shoulder at ~1210 Å^2. The distribution for the +7 *D* ions shows that two conformation types are present, a compact form at ~1050 Å^2 and a broad peak that reaches a maximum at ~1230 Å^2. The dominant feature for the +8 state for both solutions is a broad feature that peaks near ~1300 Å^2. The distribution for the +8 *N* ions also has a smaller peak at 1030 Å^2 that is due to more compact states. Under denaturing conditions, the +9 and higher states all favor conformations with large cross sections: ~1600 Å^2 (+9); ~1680 Å^2 (+10 *D*); 1720 Å^2 (+11 *D*); 1830 Å^2 (+12 *D*); and 1970 Å^2 (+13 *D*). These peaks are in excellent agreement (within 2% relative uncertainty) with cross sections for the most extended conformations formed in injected ion studies [4c]. According to the previous assignments, these large cross sections must have unfolded conformations with little tertiary structure [4c]. The +9 *D* and +10 *D* ions also show features corresponding to partially folded conformers that peak near ~1400 and 1500 Å^2, respectively. Distributions for higher charge states from the *N* solution shown in Fig. 2 (+9 to +11) and +12 (not shown), display features that are in similar positions to those observed for the *D* solution. A general trend of all charge states is that

ions formed from *N* solutions favor a larger fraction of compact and partially folded conformers than ions formed from *D* solutions.

From the relative abundances of different charge states in the mass spectra and different conformers in the cross section distributions we estimate populations for the compact, partially folded, and unfolded states of ~35%, 35%, and 30%, respectively, for the *N* solution, compared with ~3%, 30%, and 67%, respectively, for the *D* solution. The changes in these populations are far outside the estimated uncertainties of this analysis (±3 to 5%). These data show a shift from compact to unfolded states as the nonaqueous portion of the solution is increased. The changes in populations are consistent with conformations that are expected to be present in these solutions. It appears that at least some differences in the solution structures (induced by variations in solvent) are preserved during the ESI process and can be distinguished based on differences in the resulting gas-phase conformation. This interpretation of these data is consistent with suggestions that a degree of memory of the solution conformation can be preserved in the gas-phase conformation [4b,5a,7,16,17]. This should be taken cautiously, however; an equally valid explanation is that differences in the solvent systems influence the ESI process leading to a change in the gas-phase conformation. For example, differences in effectiveness of the different solvent systems to cool (and stabilize) the protein during droplet evaporation could also influence the gas-phase conformations that are formed.

The increase in cross section that is observed with increasing charge state is in good agreement with our previous injected ion measurements for ubiquitin [4c]. As discussed previously [2,5a], the increased coulomb repulsion between charges forces high charge states to adopt more open conformations. This effect should be pronounced in the gas phase [37] where the dielectric is ~1.0 and coulombic interactions are not effectively shielded by the high dielectric of the water (~80) [38]. These results are similar to data reported for cytochrome *c* [3a, 4a, 5a], apomyoglobin [5d,17], lysozyme [4b], and small DNA oligomers [32].

Finally, we also note that the features and peaks observed in these distributions are much broader than those calculated by the transport equation [39] for a single rigid conformation under the conditions of our experiment. For example, the full width at half maximum (FWHM) of peaks in the +6 N distribution is about a factor of 15 times broader than the FWHM for peak shapes calculated using the transport equation [40]. This indicates that either multiple conformations are present, or conformers interconvert as they travel through the drift tube. Broader peaks observed for the intermediate charge states (+7 to +9) indicate that a wider array of structures are present. Features that were much broader than expected for a single conformer were also observed for cytochrome *c* [16].

3.2. Influence of capillary temperature

Cross section distributions are found to be extremely sensitive to the capillary temperature that is used. Fig. 4 shows a series of cross section distributions as a function of capillary temperature for the +6 to +11 ions. These ions were formed by electrospraying a denatured (49:49:2) solution.

As the capillary temperature is increased, cross section distributions show that the +6 state favors a compact conformation until ~70 to 80 °C. Above this temperature (97 °C), three unresolved peaks from ~950 to 1430 $Å^2$ are observed. At our highest temperature (132 °C), the compact conformer disappears and an unresolved distribution of partially folded states remains. The +7 state shows many similarities to the +6 state, but transitions occur at lower temperatures. The +8 to +10 charge states all show partially folded and unfolded conformers at 25 °C. At high capillary temperatures, the fractions of compact conformers decrease and the unfolded conformers dominate the distribution. The +11 and higher charge states are each dominated by a single unfolded conformer at all temperatures. Mass spectra recorded at these capillary temperatures are all similar to data recorded at 25 °C. This indicates that the changes that are observed are due to unfolding transitions and not to thermally induced dissociation. Smith and co-workers have previously observed sig-

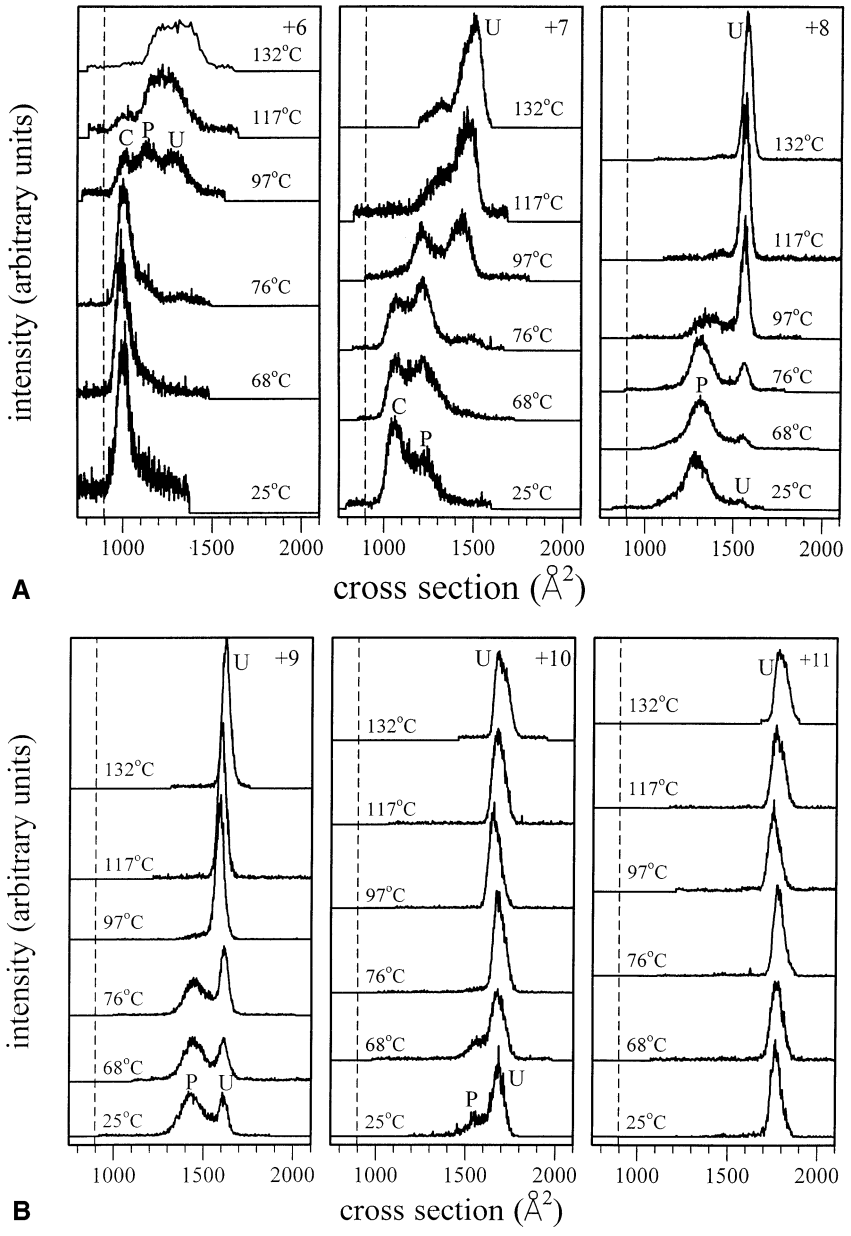

Fig. 4. Cross section distributions at capillary temperatures ranging from 25 to 132 °C for the (a) +6 to +8 charge states and (b) +9 to +11 charge states of ubiquitin obtained by electrospraying a 49:49:2 water:acetonitrile:acetic acid solution. The labels (C), (P), and (U) denote compact, partially folded, and unfolded states, respectively. The dashed line shows the calculated cross section for the crystal coordinates of ubiquitin, taken from [34].

nificant fractions of product ions from thermal dissociation at capillary temperatures above 180 °C [9a].

Fig. 5 shows the fractions of compact, partially folded, and unfolded states as a function of capillary temperature that are deduced by integration of appropriate regions of each distribution. At low capillary temperatures, the fraction of unfolded conformers is negligible for the +6 and +7 charge states and for

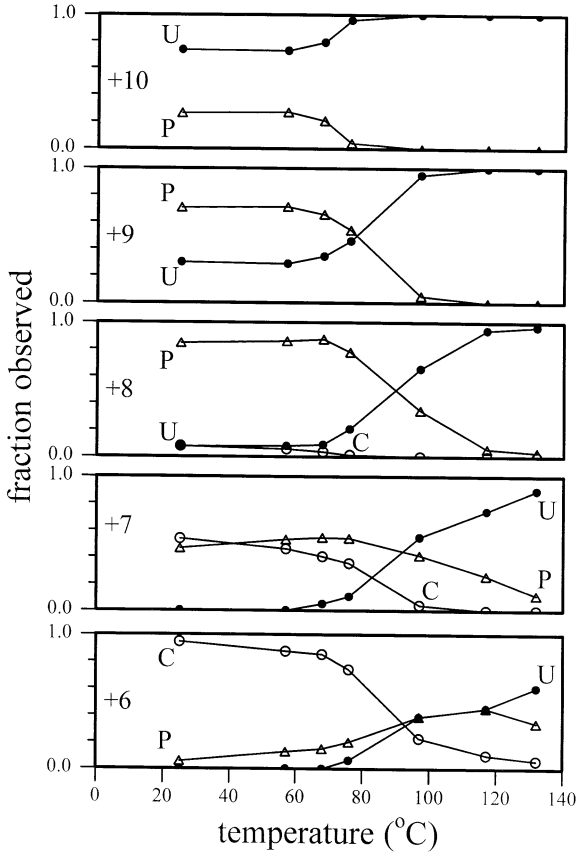

Fig. 5. Fractions of compact (C), partially folded (P), and unfolded (U) conformations for the +6 to +10 charge states as a function of capillary temperature for ESI of a 49:49:2 water:acetonitrile:acetic acid solution.

higher charge states increases with increasing charge state: ~7% (+8); 32% (+9); 76% (+10); and 100% for higher charge states. The increasing population of unfolded states (with increasing charge state) can be understood by noting that coulomb repulsion forces higher charge states to adopt unfolded conformations [3, 4]. As the capillary temperature is increased, the fractions of unfolded conformers remain essentially constant until a critical temperature. At this point, the fractions of unfolded conformations increase rapidly with temperature. The range of temperatures in the transition regions (~76 to 117 °C for the +8 ions, ~72 to 97 °C for the +9 ions, and ~68 to 80 °C for the +10 ions) decreases and sharpens with increasing charge state.

The observation that high charge states unfold at lower temperatures can be understood by considering that increased coulomb repulsion should reduce barriers associated with unfolding. Analogies can be drawn between this behavior in the gas phase and thermal denaturation of ubiquitin in solution [26]. At a pH of 5.8, ubiquitin retains its native conformation in solution from 25 to 82 °C and precipitates at higher temperatures. At a pH below 2, the unfolded state is observed at 77 °C; addition of strong denaturants such as urea or guanidinium chloride induces unfolding at lower temperatures.

Additional information regarding the unfolding pathway can also be gleaned from Fig. 5. At 25 °C, ~60% of the +7 ions are compact and 40% are partially folded. When the temperature is increased, the fraction of compact conformers decreases while the abundance of partially folded conformers increases. This shows that compact conformers are precursors to partially unfolded states. At higher temperatures (~85 to 97 °C) the fraction of partially folded conformers decreases; over the same temperature range the abundance of unfolded states increases. From this, it appears that compact conformers unfold through partially unfolded intermediates before reaching the unfolded state. Again it is possible to draw analogies between this three state system and the three states of ubiquitin that are known in solution: the native state; the A state, favored in solutions containing 60% methanol; and the unfolded state, observed at high temperatures or upon addition of strong denaturants [26].

Thermal unfolding through partially folded intermediates also has similarities to unfolding transitions in the gas phase that are observed with increasing charge state. Typically, cross sections measured as a function of charge state for proteins show a single compact conformer at low charge states; intermediate charge states display a wide array of conformations with different cross sections [3,4]. High charge states favor a narrow distribution of unfolded states. For low charge states, attractive folding interactions outweigh repulsive coulombic interactions and compact states are favored. High charge states are dominated by repulsive forces that favor unfolded states. The broad

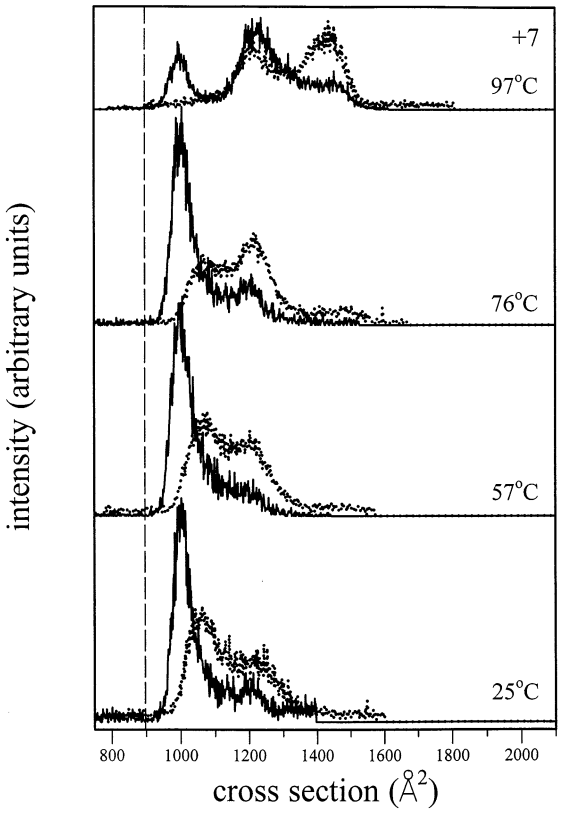

Fig. 6. Cross section distributions for the +7 charge state of ubiquitin at capillary temperatures of 25, 57, 76, and 97 °C. The solid circles represent data obtained by electrospraying a 49:49:2 water:acetonitrile:acetic acid solution. The solid lines correspond to the pseudo-native 89:9:2 water:acetonitrile:acetic acid solution. The dashed line shows the calculated cross section for the crystal coordinates of ubiquitin, taken from [34].

distribution of structures observed for intermediate charge states arises from a near balance of attractive folding and repulsive unfolding interactions. This leads to an array of partially folded forms with different cross sections.

3.3. Influence of capillary temperature upon ESI of pseudonative solutions

Fig. 6 shows cross section distributions for the +7 *N* and +7 *D* ions for a range of capillary temperatures. As mentioned above, at 25 °C the +7 *N* ions favor conformations that are more compact than both of the features observed for the +7 *D* ions. At a capillary temperature of 57 °C distributions for both solutions are similar to data at 25 °C. At 76 °C and higher temperatures the distributions of conformers shows a shift and ions with larger cross sections are favored.

It is clear from Fig. 6 that the abundance of compact conformations from the *N* solution is greater at all temperatures than the fraction of compact +7 *D* ions. This trend is similar for all charge states and suggests that compact conformers formed from *N* solutions are more stable than compact states formed from *D* solutions. In addition, the peak positions and peak shapes for ions that are formed at high temperatures are similar for the *N* and *D* solutions. This suggests that the products of thermal unfolding are the same for both solvent systems. The similarities between product conformers for the *N* and *D* solutions at high capillary temperatures can be understood by considering that thermal annealing of gas-phase ions should reduce the differences between structures that were retained from the different solvent systems. In this way, both precursor ions would be converted into states that are favored in the gas phase. It is also possible that thermal denaturation of the protein occurs before the electrosprayed droplet has dried. In this case, the electrosprayed ion denatures in solution and when the solvent evaporates both solutions yield similar gas-phase ion conformations. This latter explanation is also consistent with the observation that gas-phase conformations unfold at temperatures that are similar to those in solution as well as the similarities in three primary states observed here and in solution [26].

4. Conclusions

High-resolution ion mobility/mass spectrometry techniques have been used to study the influence of solvent composition and capillary temperature on the conformations of ubiquitin ions. These results show that source conditions (e.g. the solvent system and capillary temperature) used for ESI can have a pronounced influence on the conformations of the gas-

phase ions that are formed. Using a 25 °C capillary, cross section distributions for ions formed from pseudonative solvent systems show peaks that correspond to more compact conformers than those observed upon ESI of denatured solutions. The total population of compact conformations for all charge states is ~3% for ESI of denatured solutions and ~35% for compact ions formed from more aqueous solutions. Studies as a function of capillary temperature show that compact and partially folded conformers unfold at high temperatures. For the +7 state (electrosprayed from denatured solutions) the transition appears to occur through a partially folded intermediate. Overall, compact states formed from pseudonative solutions require higher temperatures for unfolding than compact conformations formed from denatured solutions. This difference may be due to variations in solution environment as the electrosprayed droplet dries or to differences in the stabilities of the two compact ion forms in the gas phase.

Acknowledgements

This work is supported by the National Science Foundation (grant no CHE-9625199) with additional support from the Petroleum Research Fund administered by the ACS (grant no ACS-PRF 31859-G4). J.W.L. wishes to thank Stephen J. Valentine for instruction in data collection and analysis. The authors are also grateful to Mike Freidas and Alan Marshall for sharing their preliminary hydrogen/deuterium exchange results.

References

[1] Ion mobility spectrometry methods are discussed in the following references: (a) D.F. Hagen, Anal. Chem. 51 (1979) 870. (b) J.C. Tou, G.U. Boggs, *ibid*. 48 (1976) 1351. (c) Z. Karpas, M.J. Cohen, R.M. Stimac, R.F. Wernlund, Int. J. Mass Spectrom. Ion Processes 83 (1986) 163. (d) R.H. St. Louis, H.H. Hill, Crit. Rev. Anal. Chem. 21 (1990) 321. (e) G. von Helden, M.T. Hsu, P.R. Kemper, M.T. Bowers, J. Chem. Phys. 95 (1991) 3835. (f) M.F. Jarrold, J. Phys. Chem. 99 (1995) 11.

[2] For recent reviews of ion mobility studies of biomolecules, see: D.E. Clemmer, M.F. Jarrold, J. Mass Spectrom. 32 (1997) 577. Y. Liu, S.J. Valentine, A.E. Counterman, C.S. Hoaglund, D.E. Clemmer, Anal. Chem. 69 (1997) 728A.

[3] (a) D.E. Clemmer, R.R. Hudgins, M.F. Jarrold, J. Am. Chem. Soc. 117 (1995) 10141. (b) K.B. Shelimov, D.E. Clemmer, R.R. Hudgins, M.F. Jarrold, *ibid*. 119 (1997) 2240. (c) K.B. Shelimov, M.F. Jarrold, *ibid*. 119 (1997) 9586.

[4] (a) S.J. Valentine, D.E. Clemmer, J. Am. Chem. Soc. 119 (1997) 3558. (b) S.J. Valentine, J. Anderson, A.E. Ellington, D.E. Clemmer, J. Phys. Chem. B 101 (1997) 3891. (c) S.J. Valentine, A.E. Counterman, D.E. Clemmer, J. Am. Soc. Mass Spectrom. 8 (1997) 954.

[5] (a) T.R. Covey, D.J. Douglas, J. Am. Soc. Mass Spectrom. 4 (1993) 616. (b) K.A. Cox, R.K. Julian, R.G. Cooks, R.E. Kaiser, *ibid*. 5 (1994) 127. (c) Y.-L. Chen, B.A. Collings, D.J. Douglas, *ibid*. 8 (1997) 681. (d) B.A. Collings, D.J. Douglas, J. Am. Chem. Soc. 118 (1996) 4488. (e) Y.-L. Chen, B.A. Collings, D.J. Douglas, J. Am. Soc. Mass Spectrom. 8 (1997) 681.

[6] I.A. Kaltashov, C.C. Fenselau, J. Am. Chem. Soc. 117 (1995) 9906. J. Adams, F. Strobel, A. Reiter, J. Am. Soc. Mass Spectrom. 7 (1996) 30. I.A. Kaltashov, C.C. Fenselau, Proteins, 27 (1997) 165.

[7] P.A. Sullivan, J. Axelsson, S. Altmann, A.P. Quist, B.U.R. Sunqvist, C.T. Reimann, J. Am. Soc. Mass Spectrom. 7 (1996) 329.

[8] D.S. Gross, P.D. Schnier, S.E. Rodriguez-Cruz, C.K. Fagerquist, E.R. Williams, J. Am. Chem. Soc. 31 (1996) 831.

[9] (a) B.E. Winter, K.J. Light-Wahl, A.L. Rockwood, R.D. Smith, J. Am. Chem. Soc. 114 (1992) 5897. (b) D. Suckau, Y. Shi, S.C. Beu, M.W. Senko, J.P. Quinn, F.M. Wampler, F.W. McLafferty, Proc. Natl. Acad. Sci. U.S.A. 90 (1993) 790.

[10] C.J. Cassady, S.R. Carr, J. Mass Spectrom. 93 (1996) 3143.

[11] M. Freitas, A.G. Marshall, Int. J. Mass Spectrom. 182–183 (1999) 221.

[12] P.F. Schnier, D.S. Gross, E.R. Williams, J. Am. Chem. Soc. 117 (1995) 6747. E.R. Williams, J. Mass Spectrom. 31 (1996) 831.

[13] S.E. Rodriguez-Cruz, J.S. Klassen, E.R. Williams, J. Mass Spectrom. 8 (1997) 565.

[14] J.L. Fye, J. Woenckhaus, M.F. Jarrold, J. Am. Chem. Soc. 120 (1998) 1327.

[15] J.B. Fenn, M. Mann, C.K. Meng, S.F. Wong, C.M. Whitehouse, Science 246 (1989) 64.

[16] R.R. Hudgins, J. Woenckhaus, M.F. Jarrold, Int. J. Mass Spectrom. Ion Processes 165/166 (1997) 497.

[17] K.B. Shelimov, M.F. Jarrold, J. Am. Chem. Soc. 119 (1997) 2987.

[18] S.K. Chowdhury, V. Katta, B.T. Chait, J. Am. Chem. Soc. 112 (1990) 9012.

[19] J.A. Loo, R.R. O. Loo, H.R. Udseth, C.G. Edmonds, R.D. Smith, Rapid Commun. Mass Spectrom. 5 (1991) 101.

[20] U.A. Miraz, S.L. Cohen, B.T. Chait, Anal. Chem. 65 (1993) 1.

[21] J.C.Y. LeBlanc, D. Beuchemin, K.W.M. Siu, R. Guevremont, S.S. Berman, Org. Mass Spectrom. 5 (1991) 582.

[22] A.S. Rockwood, M. Busman, H.R. Udseth, R.D. Smith, Rapid Commun. Mass Spectrom. 5 (1991) 582.

[23] G. Goldstein, M. Scheid, U. Hammerling, E.A. Boyse, D.H. Schlesinger, H.D. Niall, Proc. Natl. Acad. Sci. 72 (1975) 11.
[24] R.E. Lenkinski, D.M. Chen, J.D. Glickson, G. Goldstein, Biochem. Biophys. Acta. 494 (1977) 126.
[25] P.D. Cary, D.S. King, C. Crane-Robinson, E.M. Bradbury, A. Rabbani, G.A. Goodwin, E.W. Johns, Eur. J. Biochem. 112 (1980) 577.
[26] M.M. Harding, D.H. Williams, D.N. Woolfson, Biochemistry 30 (1991) 3120.
[27] X. Zhang, C.J. Cassady, J. Am. Soc. Mass Spectrom. 7 (1996) 1211.
[28] (a) D. Wittmer, Y.H. Chen, B.K. Luckenbill, H.H. Hill, Jr., Anal. Chem. 66 (1994) 2348. (b) Y.H. Chen, H.H. Hill, Jr., D.P. Wittmer, Int. J. Mass Spectrom. Ion Processes 154 (1996) 1. (c) R. Guevremont, K.W.M. Siu, J. Wang, L. Ding, Anal. Chem. 69 (1997) 3959.
[29] Equipotential lines were calculated using: SIMION 3D, Idaho National Engineering Laboratory, Idaho Falls, ID (1994).
[30] A.E. Counterman, S.J. Valentine, C.A. Srebalus, S.C. Henderson, C.S. Hoaglund, D.E. Clemmer, J. Am. Soc. Mass Spectrom. 9 (1998) 743.
[31] C.S. Hoaglund, D.E. Clemmer, unpublished.
[32] C.S. Hoaglund, Y. Liu, M. Pagel, A.D. Ellington, D.E. Clemmer, J. Am. Chem. Soc. 119 (1997) 9051.
[33] G. von Helden, T. Wyttenbach, M.T. Bowers, Science 267 (1995) 1483. T. Wyttenbach, G. von Helden, M.T. Bowers, J. Am. Chem. Soc. 118 (1996) 8355.
[34] The crystal coordinates for human ubiquitin (having the same sequence as bovine ubiquitin) were used for this calculation. The structure was determined by S. Vijay-Kumar, C.E. Bugg, W.J. Cook, J. Mol. Biol. 194 (1987) 531.
[35] T. Wyttenbach, G. von Helden, J.J. Batka, Jr., D. Carlat, M.T. Bowers, J. Am. Soc. Mass Spectrom. 8 (1997) 275.
[36] A.A. Shvartsburg, M.F. Jarrold, Chem. Phys. Lett. 261 (1996) 86. M.F. Mesleh, J.M. Hunter, A.A. Shvartsburg, G.C. Schatz, M.F. Jarrold, J. Phys. Chem. 100 (1996) 16082.
[37] S.F. Wong, C.K. Meng, J.B. Fenn, J. Phys. Chem. 92 (1988) 546. T. Nohmi, J.B. Fenn, J. Am. Chem. Soc. 114 (1992) 3241. A.L. Rockwood, M. Busman, R.D. Smith, Int. J. Mass Spectrom. Ion Processes 111 (1991) 103.
[38] R.C. Weast (Ed.), Handbook of Chemistry and Physics, CRC, Boca Raton, FL, 1985.
[39] E.A. Mason, E.W. McDaniel, Transport Properties of Ions in Gases, Wiley, New York, 1988.
[40] Although these peaks are broader than expected for a single conformer, there is still a small improvement in resolution compared with injected ion studies (about a factor of 2 to 3). We have observed peaks comparable to the width of the calculated distributions for smaller systems. See [30].